Retinal Remodeling in a Rat Model of the Smith-Lemli-Opitz Syndrome (SLOS)

Steven J. Fliesler[1,2], Christopher C. Goulah[1,2], W. Drew Ferrell[3], Robert E. Marc[3], & Bryan W. Jones[3]

[1]Research Service, VAWNYHS, Buffalo, NY; [2]Ophthalmology & Biochemistry/ SUNY-Buffalo and SUNY Eye Institute, Buffalo, NY, USA

[3]Department of Ophthalmology, Moran Eye Center, University of Utah, Salt Lake City, UT, USA

PURPOSE

Smith-Lemli-Opitz syndrome (SLOS) is a developmental disorder involving defective cholesterol biosynthesis. Prior studies using a rat model of SLOS have documented progressive retinal dysfunction and degeneration, apparently involving caspase-3-independent cell death of photoreceptors. Retinal remodeling has been documented in human retinal degenerations and a myriad of animal models of retinal disease (*Jpn J Ophthalmol.* 56(4):289, 2012). Here, we examined retinal degeneration and remodeling in the SLOS rat model vs. age-matched control rats.

METHODS

A pharmacologically-induced rat model of SLOS was generated by treating Sprague-Dawley rats with AY9944 (*Arch. Ophthalmol.* 122:1190, 2004). At 81 days postnatal (P81), eyes from AY9944-treated and control rats were enucleated, fixed in buffered mixed aldehydes, and processed for computational molecular phenotyping (CMP) (*J Neurosci.* 15:5106, 1995; *J Comp Neurol.* 464:1, 2003).

BACKGROUND

The AY9944-Induced SLOS Rat Model

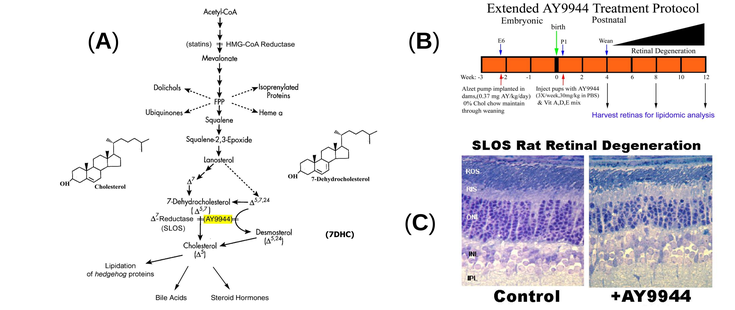

Figure 1. (**A**) AY9944 blocks sterol synthesis at the level of 3β–dehydroxysterol-Δ7-reductase (DHCR7), resulting in build-up of 7DHC and reduced levels of cholesterol in all tissues, as occurs in the Smith-Lemli-Opitz syndrome (SLOS). (**B**) Timeline of AY9944 treatment protocol and tissue harvest (**C**) Histology of control (left) and AY9944-treated (right) rat retinas at 3 mo, illustrating the retinal degeneration: reduced outer nuclear layer (ONL) thickness, increased ONL pyknosis, and shortened outer segment length (relative to control). At this age, SLOS rats also exhibit concomitant ERG deficits (decreased rod and cone ERG amplitudes and increased implicit times), relative to age-matched controls (not shown; Fliesler et al., *Arch. Ophthalmol.* 122:1190, 2004).

Computational Molecular Phenotyping (CMP)

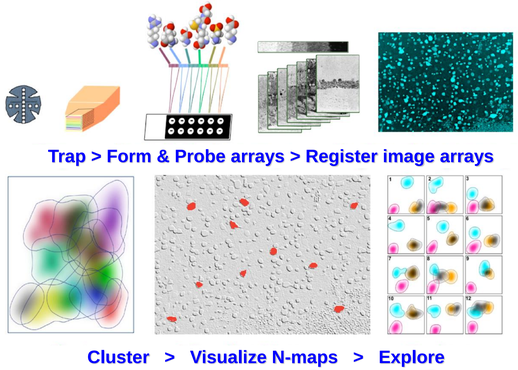

Figure 2. Standard mixed aldehyde-fixed, plastic resin-embedded rat retinas were sectioned by ultramicrotomy into serial arrays of 200 nm thickness on multiwell slides and each well was simultaneously probed with IgGs from a library targeting a spectrum of micro-molecules, including aspartate [**D**], *gamma*-aminobutyrate (GABA, γ), glycine [**G**], glutamate [**E**], glutamine [**Q**] taurine [**T**], and stained with DAPI to reveal structure. Signals were visualized with silver detection and digitally captured; the images of molecular signals were then registered as data arrays at ≈ 200 nm precision, with every pixel locus indexing a chemical vector in N-dimensional space.

RESULTS

CMP of SLOS model (AY9944-treated) retinas reveals progressive retinal degeneration with loss of rod and cone photoreceptors (PRs), although by P81, PR degeneration is not complete, since some rod/cone PRs remain. Spikes in aspartate concentration indicative of "cell stress/death" can be seen in patches of PRs. Aberrant sprouting of glycinergic amacrine cells (ACs) is observed, as well as large stretches in the peripheral retina bereft of glycinergic or GABAergic ACs. Punctate glutamate signals in the middle of the PR layer suggest aberrantly sprouting bipolar cells or PR processes. Müller cells also exhibit early signs of hypertrophy, plasticity and early formation of the Müller cell seal with patchy up-regulation in glutamine and glutathione signals, consistent with prior observations of dramatic up-regulation of GFAP and gliosis in this model. DAPI labeling also shows non-uniform nuclear staining density (pyknosis) in populations of PRs and bipolar cells, consistent with the observed loss of PRs and retinal thinning.

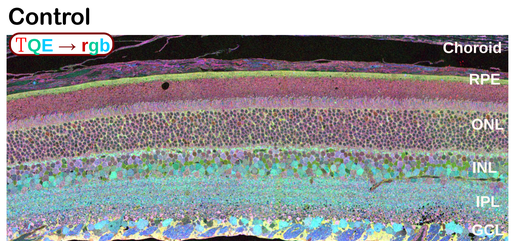

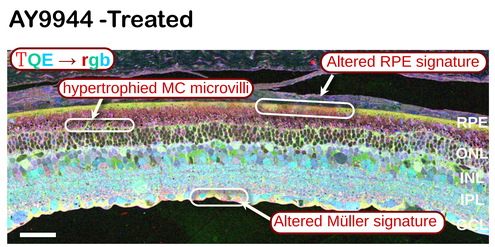

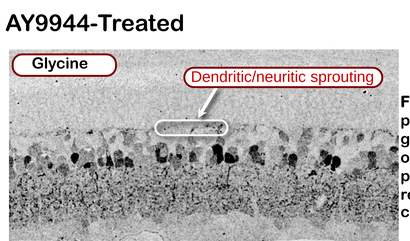

Figure 6. Imaging of glycinergic (GLYT-1 -positive) amacrine cells (ACs). Far greater numbers of such cells are observed sprouting into the outer plexiform layer (OPL) in AY9944-treated retinas, compared to normal age-matched control retinas. Scale bar, 30 μm.

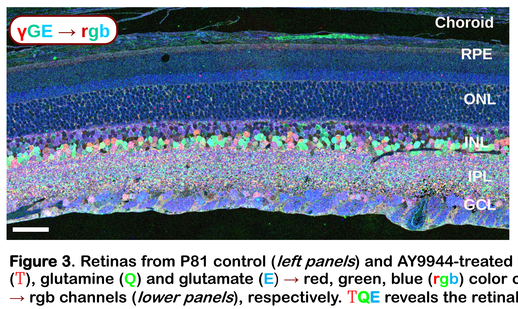

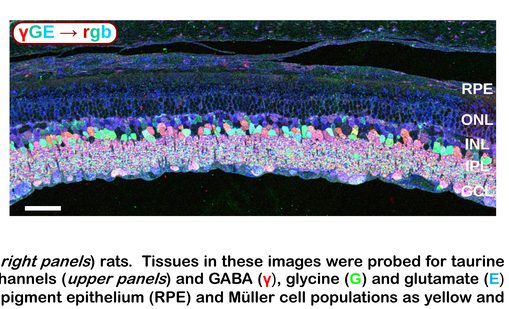

Figure 3. Retinas from P81 control (*left panels*) and AY9944-treated (*right panels*) rats. Tissues in these images were probed for taurine (T), glutamine (Q) and glutamate (E) → red, green, blue (rgb) color channels (*upper panels*) and GABA (γ), glycine (G) and glutamate (E) → rgb channels (*lower panels*), respectively. TQE reveals the retinal pigment epithelium (RPE) and Müller cell populations as yellow and gold, while γGE reveals the excitatory and inhibitory neuronal populations. Photoreceptor cell death and loss is evident as revealed by thinning of the ONL and initial evidence of Müller hypertrophied microvilli can be observed in the AY9944 treated retina on the right. Additionally, RPE dysfunction is observed with variations in RPE signatures, as normally RPE cells are extensively coupled and all signatures should be identical. Müller cell signatures are also observed as becoming altered with up-regulation of taurine and glutamine suggesting local response to retinal degenerative events. Slight evidence can also be seen for glycinergic and GABAergic amacrine sprouting in the γGE images, but is better revealed in the γG image to the right. Scale bar, 52 μm.

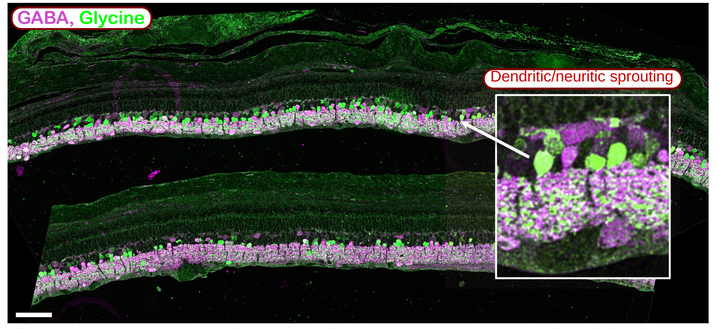

Figure 7. Imaging of glycine (*green*) and GABA (*magenta*) signals in a P81, AY9944-treated rat retina. Note the dramatic loss of both glycinergic and GABAergic amacrine cells (ACs) from the peripheral retina (*upper section*) to central retina (*lower section*). Arbors of sprouting glycinergic and GABAergic processes also can be observed projecting vertically into the OPL, far in excess of normal numbers of glycinergic (GLYT-1–positive) ACs. Additionally, some profiles are GABAergic and unrelated to horizontal cell processes. Scale bar, 52 μm.

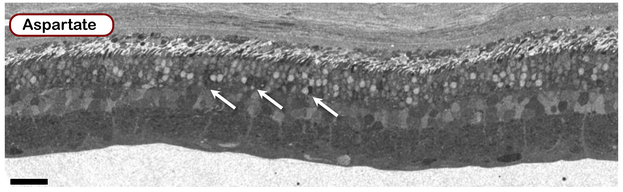

Figure 4. Aspartate labeling (density scaled) in the AY9944 treated rat retina shows aberrant signals with aspartate spikes (*arrows*) in some rod patches next to rod patches with aberrant aspartate loss. Elevated aspartate signals appear to be an early stress marker in photoreceptors and occur panretinally. The mechanism for this is unknown, but suggests dysfunction in the aspartate-malate shuttle. Scale bar, 30 μm.

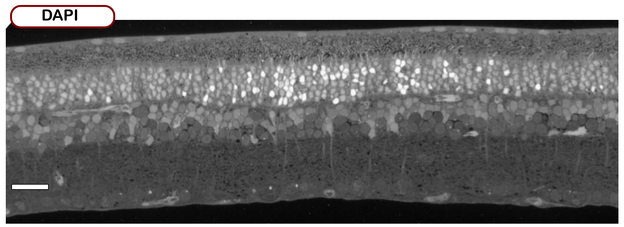

Figure 5. DAPI (intensity-scaled) labeling shows variation in the nuclear intensity suggesting different pyknotic states, mostly in photoreceptors, but also observed in bipolar cell populations. These signals are metabolically complex and do not necessarily correlate with high aspartate levels, but do correlate with up-regulation of GFAP and Müller cell gliosis. Scale bar, 30 μm.

CONCLUSIONS

Retinal remodeling, involving early retinal restructuring of both neuronal and glial populations, occurs in the AY9944-induced rat model of SLOS and is consistent with previous observations concerning retinal dysfunction and pathology in this model. Additionally, the large variations in DAPI labeling among photoreceptor and bipolar cell populations suggests large variations in DNA accessibility and, thus, gene expression, consistent with prior observations in this SLOS rat model.

This work was supported, in part, by U.S.P.H.S. (NEI/NIH) grants EY007361, EY002576, EY015128, EY014800 (Vision Core), by NSF grant 0941717, by facilities and resources provided by the Veterans Administration Western New York Healthcare System (SJF), by Unrestricted Grants from Research to Prevent Blindness (RPB) to the Depts of Ophthalmology (SUNY-Buffalo and Univ. of Utah), by an RPB Career Development Award (BWJ), and by a Thome Memorial Foundation Grant for AMD (BWJ).